Biometals (2010) 23:1191–1201
DOI 10.1007/s10534-010-9369-2

Effect of Ni^{2+} and Cd^{2+} ions on thermally induced conformational transitions in poly(dA)-poly(dT) system

Victor N. Zozulya · Olga A. Ryazanova · Nataliya N. Zhigalova · Yurii P. Blagoi

Received: 18 March 2010 / Accepted: 23 July 2010 / Published online: 6 August 2010

Abstract Effects of Ni^{2+} and Cd^{2+} ions on thermally induced conformational transitions in the poly(dA)·poly(dT) polynucleotide duplex and poly(dA)·2poly(dT) triplex under near physiological ionic conditions were studied by measurement of UV absorption melting curves and static light scattering intensity. The diagrams of conformational transitions in poly(dA)-poly(dT)-Me^{2+} systems were plotted. An aggregation in these polynucleotide systems arises at certain values of the metal ions concentration and the temperature after the polymer dissociation into single strands. The phenomenon is conditioned by the aggregation of poly(dA) via the interstrand cross-linking by the dication bridges. Unlike Ni^{2+}, Cd^{2+} induces formation of very stable aggregates which did not disintegrate even upon cooling up to room temperature.

Keywords $Ni^{2+} \cdot Cd^{2+} \cdot$ Poly(dA)-poly(dT) system · Conformational transitions · Aggregation of poly(dA)

V. N. Zozulya (✉) · O. A. Ryazanova · Y. P. Blagoi
Department of Molecular Biophysics, B.Verkin Institute for Low Temperature Physics & Engineering of NAS of Ukraine, 47 Lenin ave, 61103 Kharkov, Ukraine
e-mail: zozulya@ilt.kharkov.ua

N. N. Zhigalova
Department of Biological and Medical Physics, V.N. Karazin Kharkov National University, 4 Svobody sq, 61077 Kharkov, Ukraine

Introduction

Steady contamination of the environment by transition and heavy metal compounds results in their accumulation by human and induces sharp growth of mutations and oncologic diseases. In particular, it was found that nickel and cadmium compounds, which are some of widespread urban polluting agents, induce strong carcinogenic, teratogenic, genotoxic and mutagenic effects (IARC Monographs on the Evaluation of Carcinogenic Risk to Humans 1990, 1993; Kasprzak et al. 2003; Waalkes 2000; Costa 1996; Waalkes and Misra 1996; Seoane and Dulout 2001). It was shown that prolonged exposure of nickel compounds causes lung cancer, asthma, heart and liver damage in humans. The most carcinogenic activity has insoluble compounds, namely, nickel oxides and subsulfide, whereas metallic nickel shows no carcinogenic activity. The data on water-soluble compounds are ambiguous and contradictory. They are supposed to reinforce the effect of other carcinogens. Another polluting agent, cadmium (as well as its water soluble salts), is considered to be a multitarget toxicant which ingress into human's organism from contaminated air and foods, have extremely low rate of excretion that results in its accumulation mainly in the liver and kidney. Cadmium causes lung damage, kidney disease, brittle bones and can irritate the gastrointestinal tract.

To elucidate the molecular mechanisms of Ni^{2+} and Cd^{2+} negative effects on human a number of

experimental studies was carried out on the cellular and molecular levels (Filipic et al. 2006; Kasprzak et al. 1997; Salnikow et al. 1994; Beyersmann and Hartwig 2008). It was found that strong mutagenic effect of both nickel and cadmium ions is conditioned by their ability to generate reactive oxygen species which induce oxidative DNA damages and cell deaths (Huang et al. 1994; López et al. 2006; Kim and Soh 2009), as well as to inhibit the DNA repair (Dally and Hartwig 1997; Hartwig 1994), to affect the DNA replication and gene expression (Lee et al. 1995; Sirover and Loeb 1976), that results in decrease of genetic stability and increases the probability of mutations. These ions induce chromosomal aberrations (Conway and Costa 1989; Costa and Klein 1999), cause hypermethylation of DNA and condensation of the chromatin that leads to the transition of normal cells into cancer ones. It can be noted that the negative effect of Cd^{2+} ions on human is substantially more dramatic in comparison with Ni^{2+} one. However, up to now the question regarding mechanism of Ni^{2+} and Cd^{2+} negative action is not clarified completely. To shed light on the problem the several sub-problems must be solved. In particular, the effect of these ions on the structure, function and stability of nucleic acids (NA) which are carrier of genetic information must be elucidated in detail.

Earlier an interaction of Ni^{2+} and Cd^{2+} ions with NA were investigated in vitro mainly on DNA containing systems (Eichhorn and Shin 1968; Duguid et al. 1993; Duguid et al. 1995; Aich et al. 1999; Kasyanenko et al. 1989; Sorokin et al. 1997) and polyribonucleotide ones formed by poly(rA) with poly(rU) (Sorokin et al. 2001, 2008). It was shown that these ions affect the biopolymer secondary structure and stability. Like Mg^{2+}, both Ni^{2+} and Cd^{2+} bind to oxygen of phosphate groups of the DNA or polynucleotides backbone, reducing electrostatic repulsion between their adjacent complementary strands that results in the stabilization of duplex, triplex and quadruplex structures. At the same time, both Ni^{2+} and Cd^{2+} ions also bind to electron-donor groups of nucleic bases that lead to destabilization of DNA (Saenger 1984). The resulting effect of these competitive interactions depends on the ion/polymer concentration ratio (Eichhorn and Shin 1968; Souza 2010).

Study of the simpler model homopolynucleotidic systems can be very useful and informative for understanding of the ion effects. For such systems the diagrams of the conformational transitions can be plotted, which gives the possibility to visualize the influence of the metal ions on the biopolymer structure and to lighten considerably the thermodynamic analysis. Such complete phase diagrams were obtained earlier for ribonucleotidic poly(rA)+poly(rU) duplex and triplex systems in the presence of Ni^{2+} (Sorokin et al. 2008; Sorokin et al. 2009) and Cd^{2+} (Sorokin et al. 2007; Blagoi et al. 2005) ions. However, only limited data are available for polydeoxynucleotide systems. In particular such data are available for alternating double-stranded copolymer poly(dA-dT)·poly(dA-dT) (Airoldi et al. 2007). Whereas the effect of Ni^{2+} and Cd^{+} on duplex and triplex systems formed by poly(dA) with poly(dT) homopolynucleotides remains unstudied in spite of the great biological significance of such systems.

It is known that homopolymer poly(dA)·poly(dT) has unique structural, mechanical, dynamic and functional properties (Nelson et al. 1987; Alexeev et al. 1987; Diekmann and Zarling 1987). Its conformation is characterized by unusual rigidity of the structure, shorter helical repeat, large positive propeller twist, increased base stacking and narrow minor groove of the double helix. It was revealed that long homopolymeric (dA·dT) tracts are widely presented in the eucariotic genomes including *Homo sapiens* one (Lustig and Petes 1984). Comparison of the observed frequencies of their occurrence in the genomes with the frequencies expected for random DNA revealed that the eucariotic genomes are enriched for homopolymeric (dA·dT) tracts, and the overrepresentation is exponential function of the tract length (Dechering et al. 1998). For example, human genomic DNA fragments containing $(dA{\cdot}dT)_n$ tracts where $n = 32$, 34 or 41 were reported (Fox 1992). Such stretches have great biological significance; in particular, they play major roles in structural organization of chromatin in nucleus, influence on the nucleosome organization (Segal and Widom 2009). Also they are very important for genome functioning, including regulation of the DNA transcription and recombination (Iyer and Struhil 1995). Thus, $(dA{\cdot}dT)_n$ tracts act as upstream promoter elements necessary for wild-type level of transcription (Iyer and Struhil 1995). Also it should be noted that intramolecular triplex structures can be formed in

these regions. So the construction of complete phase diagrame for duplex poly(dA)·poly(dT) and triplex poly(dA)·2poly(dT) systems in the presence of Ni and Cd ions under physiological ionic strength is very actual task. Earlier we have obtained such diagram in the presence of Mg^{2+} ions (Zozulya et al. 2003).

The aim of the present work was to study effect of Ni^{2+} and Cd^{2+} ions on the thermostability of double and triple helices formed by poly(dA) with poly(dT) under near physiological content of NaCl, and to plot the diagrams of the conformational transitions for these polynucleotide systems.

Materials and methods

Sodium salt of poly(dA)·poly(dT), poly(dA) and poly(dT) from Sigma Chemical Co. were used. For all experiments 5 mM sodium cacodylate buffer, pH 6.9, prepared with fresh deionized water ultra filtered from the Millipore-Q system and containing 0.1 M NaCl, was used as a solvent. The required concentrations of Ni^{2+} or Cd^{2+} ions in the sample were obtained by adding the precalculated volume of stock solution prepared from analytical grade $NiCl_2$ or $CdCl_2$ to the solvent. Polynucleotide concentrations were determined by the UV spectrophotometry (Specord UV–Vis spectrometer, VEB Carl Zeiss) at the temperature of 25°C using the following extinction coefficients (per mole of nucleotides) (Chalikian et al. 1999): $\varepsilon_{257} = 8{,}600\ M^{-1}cm^{-1}$ for poly(dA), $\varepsilon_{264} = 8{,}520\ M^{-1}cm^{-1}$ for poly(dT) and $\varepsilon_{260} = 6{,}000\ M^{-1}cm^{-1}$ for poly(dA)·poly(dT). The triplex poly(dA)·2poly(dT) was prepared by equimolar mixing of poly(dA)·poly(dT) and poly(dT) samples.

Experiments were carried out by methods of thermal denaturation and steady-state light scattering. Melting profiles for polynucleotides were obtained by registering the temperature dependences of absorbance at 260 nm. The rate of heating/cooling was 0.8°C/min and data were recorded every 0.5°C. The temperature dependence of light scattering intensity was registered at the right angle to the incident beam with a wavelength of 540 nm. The measurement techniques were described earlier (Zozulya et al. 2003). The polynucleotide concentration in the range of 0.1–0.4 mM in nucleic bases was used, while Me^{2+} ions content in the samples was gradually elevated up to 5 mM.

Results

Me^{2+} ions effects on melting of poly(dA)-poly(dT) system

Ni^{2+} effect

A set of absorption melting curves is shown in Fig. 1 for the poly(dA)·poly(dT) duplex in the presence of Ni^{2+} ions within the concentration range of 0–3 mM. As can be seen in Fig. 1, the only one sharp double helix-to-coil transition (2 → 1 transition) has been realized, which is shifted to higher temperatures with $[Ni^{2+}]$ increase. Upon cooling the reversibility of the helix-coil transition is observed under $[Ni^{2+}] \leq 2$ mM, the hysteresis between forward and return traces was approximately 2°C. However, at higher Ni^{2+} concentration an aggregation of the sample has occurred after the duplex dissociation into single strands, which is evident from the appearance of turbidity in the solution. Thus, for the sample containing 3 mM Ni^{2+} upon heating above 90°C the sharp growth of aggregates has occurred resulting in increase of the optical density (Fig. 1). When cooling, the aggregates were slowly disintegrated and after a few hours the double-stranded structure of the polymer was recovered as it was evidenced from the return of the absorption characteristics to original ones obtained before the melting. However, under $[Ni^{2+}] \geq 4$ mM the poly(dA)·poly(dT) was found to be in partially aggregated form already at room temperature. Further increase of Ni^{2+} concentration results in the polymer precipitation.

The effect of Ni^{2+} ions on the triplex system poly(dA)·2poly(dT) was studied under the conditions similar to those of poly(dA)·poly(dT). Absorption melting curves (Fig. 2) show the presence of two transitions. The melting profiles observed in the lowest part of temperature scale represent a separation of the poly(dT) Hoogsteen strand from poly(dA)·2poly(dT) triplex (the so-called triplex-duplex transition or 3 → 2), whereas the higher-temperature melting profiles manifest melting of poly(dA)·poly(dT) duplex itself (the 2 → 1 transition). The shape and position of last curves are in good agreement with those obtained for poly(dA)·poly(dT) duplex (Fig. 1). The lower value of hyperchromicity which has been observed under the 3 → 2 transition for the system without Ni^{2+} ions as compared to

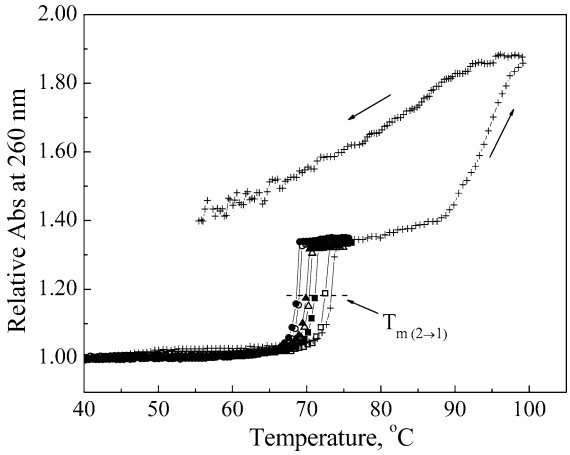

Fig. 1 Melting curves of the poly(dA)·poly(dT) duplex obtained in the presence of various Ni^{2+} concentration: 0 (*filled circle*), 0.1 (*open circle*), 0.3 (*filled triangle*), 0.6 (*open triangle*), 1 (*filled square*), 2 (*open square*) and 3 mM (*plus symbol*). The polynucleotide concentration was 0.1 mM in base pairs. The $T_{m(2 \rightarrow 1)}$ shows the 2 → 1 transition midpoint temperature. The *arrows* indicate the heating and cooling of the aggregated sample. The data points of each curve were normalized to the values at 40°C

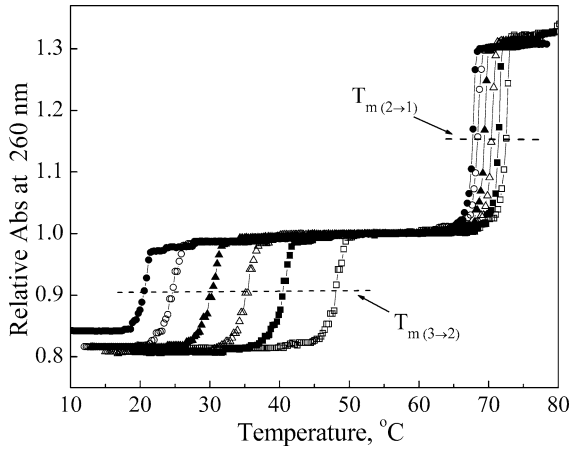

Fig. 2 Melting curves of the poly(dA)·2poly(dT) triplex obtained in the presence of various Ni^{2+} concentration: 0 (*filled circle*), 0.1 (*open circle*), 0.3 (*filled triangle*), 0.6 (*open triangle*), 1 (*filled square*) and 2 mM (*open square*). The polynucleotide concentration was 0.1 mM in base triplets. The $T_{m(2 \rightarrow 1)}$ and $T_{m(3 \rightarrow 2)}$ are 2 → 1 and 3 → 2 transition midpoint temperatures respectively. The data points of each curve were normalized to the values at 55°C

those with Ni^{2+} ions indicates the incompleteness of the triplex structure formation in the presence of 0.1 M NaCl alone. As is seen in Fig. 2, the Ni^{2+} ions elevate temperatures of both transitions however for the 3 → 2 transition this effect is essentially stronger than that for the 2 → 1 one. As well as in the case of the duplex, poly(dA)·2poly(dT) is partially aggregated even under room temperature in the presence of $[Ni^{2+}] \geq 4$ mM.

Cd^{2+} effect

As in the case of Ni^{2+} contained samples, only one sharp 2 → 1 transition was registered for poly(dA)·poly(dT) in the presence of Cd^{2+} ions (Fig. 3). However, unlike to Ni^{2+}, increase of $[Cd^{2+}]$ results in minor decrease of its midpoint temperature, $T_{m(2 \rightarrow 1)}$. It was found that this transition is reversible when $[Cd^{2+}]$ is in the range from 0 to 2 mM. The hysteresis between forward and return traces was approximately 2°C. While further addition of Cd^{2+} induces the increase of the sample absorbance after the melting of poly(dA)·poly(dT), as it is shown in Fig. 3 for the system with 4 mM Cd^{2+}. It can be explained by appearance of the solution turbidity. In this case the optical density of the sample does not change under cooling, pointing out that the double helical structure has not restored.

The effect of Cd^{2+} ions on conformational transitions in poly(dA)·2poly(dT) triplex is shown in Fig. 4. As can be seen from the figure, the addition of Cd^{2+} causes small low-temperature shift of the melting curves for 2 → 1 transition, as it was observed in the case of poly(dA)·poly(dT) duplex, but substantially enhances the thermal stability of the triplex structure. The presence of 3 or 4 mM Cd^{2+} increases the optical density at the temperature above their melting range. As in the case of the poly(dA)·poly(dT), it is caused by the rise of solution turbidity. Under the cooling to room temperature the triplex sample also remains in aggregated state. At concentrations above 5 mM Cd^{2+} ions induce an aggregation of duplex and triplex poly(dA)-poly(dT) systems already under room temperature, resulting in the partial precipitation of the sample.

Conformational transitions diagram

The effect of Ni^{2+} and Cd^{2+} ions on conformational transitions in poly(dA)-poly(dT) system is illustrated by the phase diagrams which are constructed as the plots of the transition midpoint temperatures (T_m) versus logarithm of the metal ions concentration

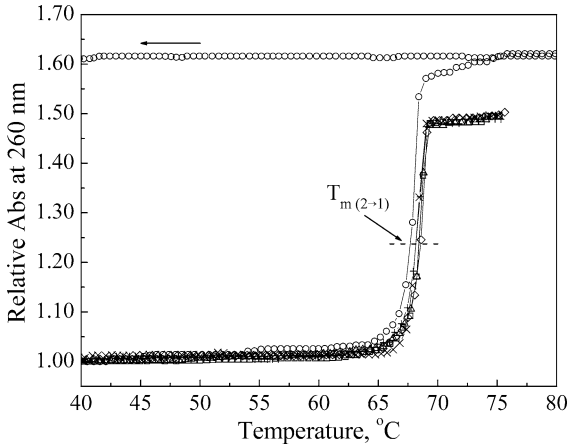

Fig. 3 Melting curves of the poly(dA)·poly(dT) duplex obtained in the presence of various Cd^{2+} concentration: 0 (*open square*), 0.2 (*open triangle*), 0.5 (*open diamond*), 1 (*plus symbol*), 2 (*cross symbol*) and 4 mM (*open circle*). The polynucleotide concentration was 0.1 mM in base pairs. The cooling of the sample containing 4 mM Cd^{2+} (*open circle*) is indicated by the *arrow*. The data points of each curve were normalized to the values at 40°C

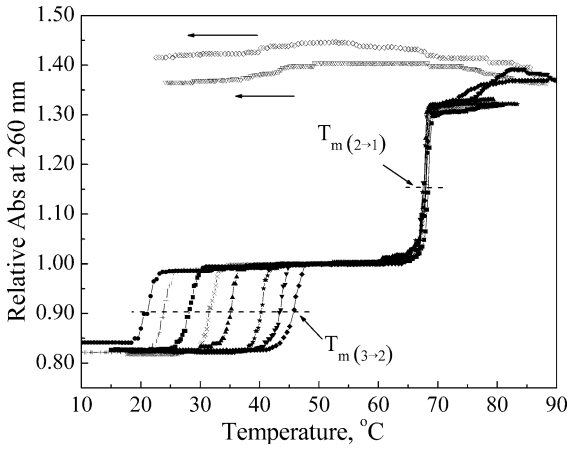

Fig. 4 Melting curves of the poly(dA)·2poly(dT) triplex obtained in the presence of various Cd^{2+} concentration: 0 (*filled circle*), 0.1 (*plus symbol*), 0.3 (*filled square*), 0.6 (*cross symbol*), 1 (*filled triangle*), 2 (*star symbol*), 3 (*filled inverted triangle*) and 4 (*filled diamond*) mM. The polynucleotide concentration was 0.1 mM in base triplets. The *arrows* indicate the cooling of the aggregated samples containing 3 (*open inverted triangle*) and 4 mM Cd^{2+} (*open diamond*). The data points of each curve were normalized to the values at 55°C

(Fig. 5). The T_m values were obtained as midpoints of absorption melting profiles for 2 → 1 ($T_{m(2 \rightarrow 1)}$) and 3 → 2 ($T_{m(3 \rightarrow 2)}$) transitions as shown in Figs. 1, 2, 3, 4, and their values were summarized

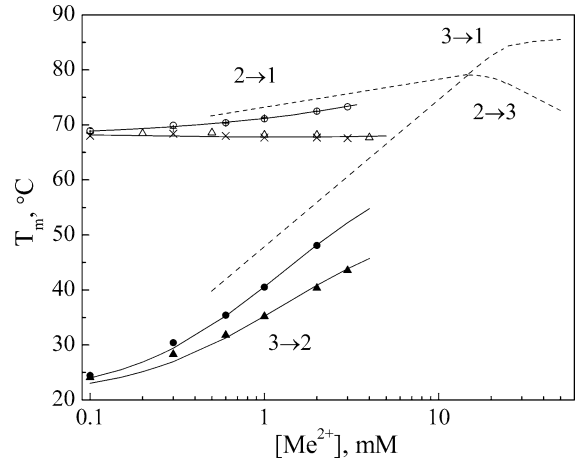

Fig. 5 Conformational transition temperature, T_m, versus divalent metal ion concentration, $[Me^{2+}]$, phase diagram for poly(dA) + poly(dT) + Me^{2+} systems in 5 mM cacodylate buffer (pH 6.9) with 0.1 M NaCl. The $T_{m(2 \rightarrow 1)}$ values were obtained from absorption profiles of poly(dA)·poly(dT) in Fig. 1 (*open circle*) and poly(dA)·2poly(dT) in Fig. 2 (*plus symbol*) for Ni^{2+} containing systems as well as from absorption profiles of poly(dA)·poly(dT) in Fig. 3 (*open triangle*) and poly(dA)·2poly(dT) in Fig. 4 (*cross symbol*) for the systems with Cd^{2+}. The $T_{m(3 \rightarrow 2)}$ data from Fig. 2 (*filled circle*) and Fig. 4 (*filled triangle*) were obtained for Ni^{2+}- and Cd^{2+}-containing systems respectively. The *dotted lines* illustrate the conformational transitions diagram for poly(dA)-poly(dT)-Mg^{2+} system (Zozulya et al. 2003)

in Table 1. It was found that the $T_{m(2 \rightarrow 1)}$ values obtained from melting of the duplex and triplex polynucleotides are in good agreement. For the comparison, the diagram of conformation transitions in poly(dA)-poly(dT)-Mg^{2+} system at the same ionic conditions (Zozulya et al. 2003) is also presented.

As can be seen from the figure, 2 → 1 branches of the conformational diagram evidence that Ni^{2+} ions elevate the thermal stability of poly(dA)·poly(dT) duplex whereas Cd^{2+} ions slightly decrease it. Thus the rise of Me^{2+} concentration up to 3 mM results in 6°C increase of $T_{m(2 \rightarrow 1)}$ in the case of Ni^{2+} and its 0.8°C decrease for Cd^{2+} one. Both Ni^{2+} and Cd^{2+} ions strongly increase the temperature of 3 → 2 transition in poly(dA)·2poly(dT) system but the Ni^{2+} effect is substantially more pronounced.

Ni^{2+} and Cd^{2+} aggregation effects

The extremely high increase in the light scattering intensity has been revealed in solutions of poly(dA)·poly(dT) and poly(dA)·2poly(dT) under $[Ni^{2+}] \geq$

Table 1 Effect of Ni^{2+} and Cd^{2+} ions on conformational transition midpoint temperatures in duplex and triplex poly(dA)·poly(dT) systems in the presence of 0.1 M NaCl

$[Me^{2+}]$, mM	$T_{m\,(2\,\rightarrow\,1)}$, °C				$T_{m\,(3\,\rightarrow\,2)}$, °C	
	poly(dA)·poly (dT) + Ni^{2+}	poly(dA)·2poly (dT) + Ni^{2+}	poly(dA)·poly (dT) + Cd^{2+}	poly(dA)·2poly (dT) + Cd^{2+}	poly(dA)·2poly (dT) + Ni^{2+}	poly(dA)·2poly (dT) + Cd^{2+}
0	68.5	67.7	68.4	68.0	20.5	20.7
0.1	68.9	68.4	–	68.0	24.5	24.1
0.2	–	–	68.45	–	–	–
0.3	70.0	69.4	–	68.4	30.4	28.3
0.5	–	–	68.6	–	–	–
0.6	70.4	70.3	–	68.0	35.4	31.8
1	71.8	71.3	68.2	67.7	40.5	35.2
2	73.3	72.5	68.2	67.7	48.1	40.35
3	74.5	–	–	67.6	–	43.54
4	–	–	67.7	–	–	–

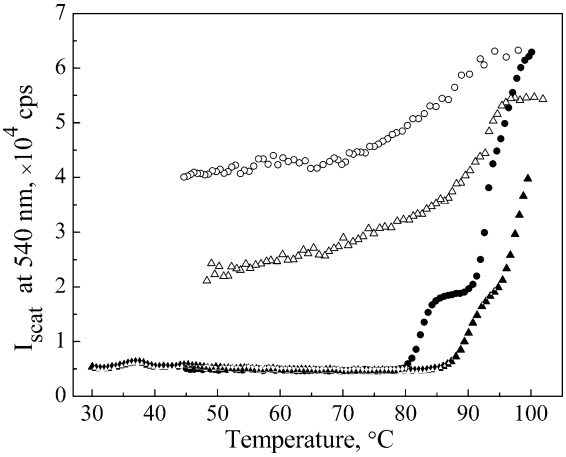

Fig. 6 Temperature dependencies of the light scattering intensity in solutions of poly(dA)·poly(dT) (0.1 mM in base pairs) with 3 mM Ni^{2+} (*open circle*, *filled circle*) and poly(dA)·2poly(dT) (0.1 mM in base triplets) with 2 mM Ni^{2+} (*filled triangle*, *open triangle*). The *filled* and *open symbols* represent the heating and the cooling curves correspondingly

2 mM and $[Cd^{2+}] \geq 4$ mM at the temperatures exceeding the range of the melting transitions (Figs. 6 and 7) recorded by the absorption changes (Figs. 1, 2, 3, 4). The phenomenon is well visually observable as a strong opalescence. It is caused by appearance of an aggregation in the systems after dissociation of duplex or triplex polynucleotides into single strands. Upon cooling the light scattering intensity data evidences that aggregates disintegrate slowly in the Ni^{2+} containing system (Fig. 6), and they do not disintegrate in the case of Cd^{2+} that follows from the constant level of the scattering (Fig. 7).

It was found that appearance of the aggregation in the above-mentioned polynucleotide systems after the melting is conditioned by an aggregation of poly(dA). Fig. 8 represents the temperature dependences of light scattering intensity measured for the single stranded polynucleotide constituents poly(dA) and poly(dT) in the presence of the investigated ions. As can be seen from this figure, for the poly(dT) sample containing Cd^{2+} the light scattering intensity is temperature-independent, whereas in the case of poly(dA) one the high concentrations of both Ni^{2+} and Cd^{2+} ions induce the sharp increase of the scattering at the temperatures above the range of poly(dA) poly(dT) melting. As seen in Fig. 8, upon cooling the aggregates disintegrate rapidly in the case

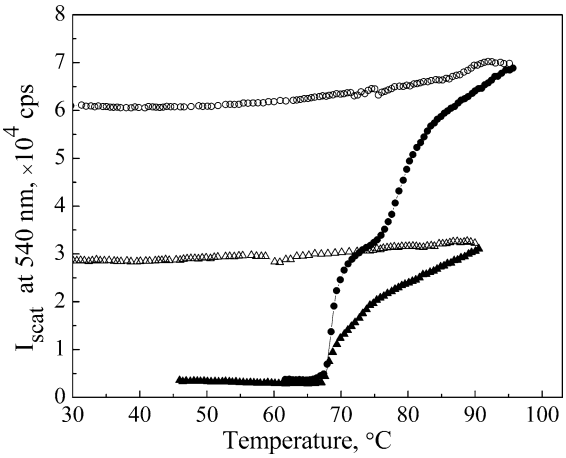

Fig. 7 Temperature dependencies of light scattering intensity in solutions of poly(dA)·poly(dT) (0.2 mM in base pairs) with 4 mM Cd^{2+} (*filled circle*, *open circle*) and poly(dA)·2poly(dT) (0.1 mM in base triplets) with 4 mM Cd^{2+} (*filled triangle*, *open triangle*). The *filled* and *open symbols* represent the heating and the cooling curves correspondingly

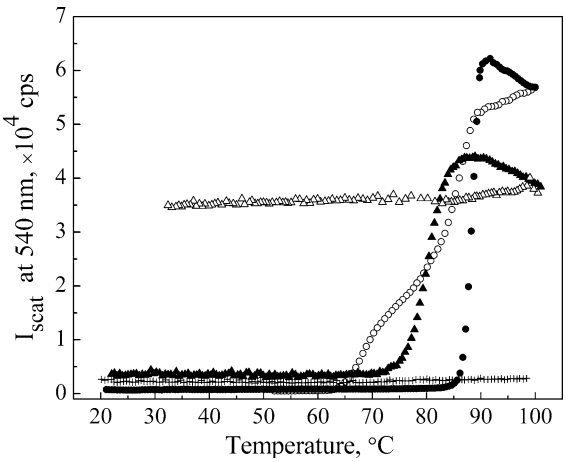

Fig. 8 Temperature dependencies of light scattering intensity in solutions of poly(dA) with 3 mM Ni^{2+} (*filled circle*, *open circle*), poly(dA) with 4 mM Cd^{2+} (*filled triangle*, *open triangle*) and poly(dT) with 4 mM Cd^{2+} (*plus symbol*). The concentrations of poly(dA) and poly(dT) were 0.1 mM in nucleic bases

of Ni^{2+}, and they are thermostable in the case of Cd^{2+}, they don't disrupt even at room temperature.

We have evaluated the size of the poly(dA)-Cd^{2+} aggregates from the data of solution turbidity applying the method of Doty and Steiner (1950), namely, using the equation:

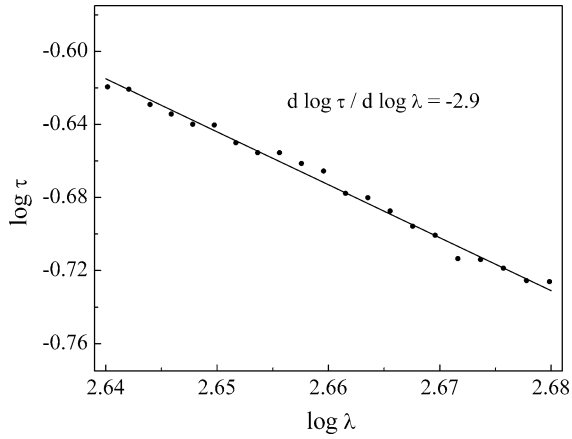

Fig. 9 Wavelength dependence of the solution turbidity measured for the poly(dA) + 4 mM Cd^{2+} system in the range of $\lambda = 435$–480 nm. The concentration of poly(dA) was 0.15 mM in nucleic bases

$$-\frac{d\log\tau}{d\log\lambda} = 4 - \frac{d\log Q}{d\log\lambda} = 4 - \beta \qquad (1)$$

where τ denotes the turbidity, Q is the particle dissipation factor and λ is the wavelength of the light in vacuum. The dependence of τ on λ was registered for the solution consisting of 0.15 mM poly(dA) and 4 mM Cd^{2+} at room temperature by measuring the absorbance in the range of $\lambda = 435$–480 nm, where poly(dA) does not absorb. From the rectilinear plot of $\log\tau$ versus $\log\lambda$ a value $\frac{d\log\tau}{d\log\lambda} = -2.9$ (Fig. 9) was calculated which determines the magnitude $\beta = 1.1$ in the Eq. (1). It is most probably that the aggregates adopt a configuration of the monodisperse coils. Under this assumption, from the Table VII (Doty and Steiner 1950) it is followed that the calculated β value corresponds to the ratio $D/\lambda' = 0.72$, where D is the coil diameter and λ' is the mean value of light wavelength in water solution over the measured wavelength range. In our case of $\lambda' \approx 340$ nm, it appears that diameter of coils is $D \approx 240$ nm.

Also the molecular weight of the poly(dA)-Cd^{2+} aggregates, M, was roughly estimated using the relationship from Doty and Steiner (1950) which was simplified in the case of low polymer concentration to:

$$H(c/\tau)Q \approx 1/M, \qquad (2)$$

where c is the weight concentration of the particles and H is the solution optical constant expressed by the formula:

$$H = 32\pi^2 n_0^2 / 3N\lambda^4 (dn/dc)^2, \quad (3)$$

where n_0 is the refractive index of the water, N is the Avogadro constant. The refractive index increment dn/dc is taken to be equal to its value for poly(rA) (Thrierr and Leng 1972), namely 0.164 ml/g. The value of H was found to be equal to $\approx 2 \times 10^{-6}$ cm^2 mol/g^2.

The weight concentration of aggregates c was calculated using molecular weights of AMP and Cd^{2+}. Because of the greate excess of Cd^{2+} in the solution one could consider that the binding of these dications to the polymer phosphate and adenine N7 sites is saturated, that gives the poly(dA)/Cd^{2+} molar ratio for the aggregate of about 1. Based on this assumption and using molecular weight of the monomeric units AMP + Cd^{2+}, $m = 442$, the value of $c = 0.66 \times 10^{-4}$ g/cm^3 was calculated in the case of [poly(dA)] = 0.15 mM. Using the Table VII in (Doty and Steiner 1950) the Q value for monodisperse coils corresponding to $\beta = 1.1$ was found to be equal 0.35. The calculation of the aggregate molecular weight fullfield for $\lambda = 450$ nm where $\tau = 0.22$ (Fig. 9) gave $M \approx 4.7 \cdot 10^9$ Da. Thus, a number of the monomeric units in the aggregate is $M/m \sim 10^7$.

It is known that in living cells relatively high intracellular content of magnesium ions is presented. They are bound to DNA phosphate backbone and can effect on the binding of transition metal ions. To evaluate the effect of Mg^{2+} ions on Ni^{2+} induced aggregation in investigated polynucleotide systems, temperature dependencies of the light scattering intensity for poly(dA)·poly(dT) and poly(dA) samples containing 3 mM Ni^{2+} were additionally recorded in the presence of 13 mM Mg^{2+} (Fig. 10). The concentration of adenine bases in both cases was 0.1 mM. As it can be seen from the comparison of Fig. 10 with Figs. 6 and 8, the presence of magnesium ions under the concentration that corresponds their content in human intracellular fluid doesn't effect substantially on Ni^{2+} induced aggregation in duplex poly(dA)·poly(dT) and single-stranded poly(dA) polynucleotide systems. Under the same concentration of nickel ions equal to 3 mM, steep melting curves corresponding changes in the light scattering intensity for both these systems turn out to be only slightly shifted to lower temperatures. For example, for poly(dA) sample the value of the shift is only 2°C. However, the presence of Mg^{2+} ions induces some change of the melting curves shape in the high-temperature region.

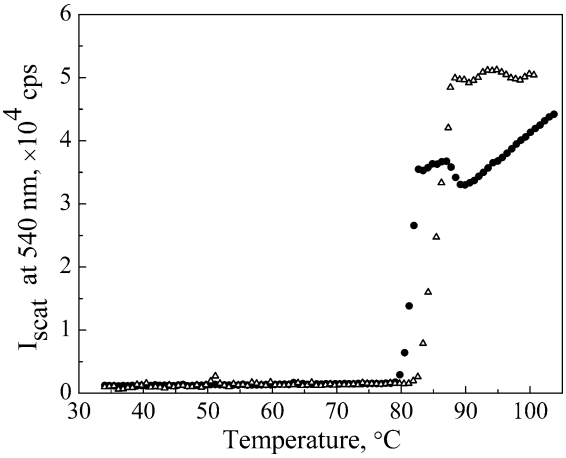

Fig. 10 Temperature dependencies of the light scattering intensity in solutions of poly(dA)·poly(dT) (*filled circle*) and poly(dA) (*open triangle*) in the presence of 3 mM Ni^{2+} and 13 mM Mg^{2+}. The concentration of adenine bases in both samples was 0.1 mM

Discussion

As can be seen from the phase diagram presented in Fig. 5, the branch corresponding to 2 → 1 transition for Ni^{2+} containing system lies very close to that for Mg^{2+}. Thus it seems clear that like Mg^{2+}, the main mechanism of Ni^{2+} ions binding to poly(dA)·poly(dT) is their chelation by phosphate groups of the polynucleotide that stabilizes the duplex structure. Whereas for Cd^{2+} ions the interaction with purine nucleic bases (in our case with N7 atoms of adenines) is also occurred (Duguid et al. 1993; Duguid et al. 1995) which disrupts the base pairing, although this effect is nearly compensated by their binding to the phosphates.

Like Mg^{2+}, the Ni^{2+} and Cd^{2+} ions sharply increase $T_{m(3 \rightarrow 2)}$ because only electrostatic binding with the polyphosphate backbone is occurred for the triplex system, whereas the interaction with nucleic bases is absent since the main acceptor sites, namely N7 atoms of poly(dA), are occupied by the Hoogsteen hydrogen bonds with poly(dT) strand. It can be noted that in contrast to the case of Mg^{2+}, the branches corresponding to 2 → 1 and 3 → 2 transitions do not reach the intersection point corresponding to equal

stabilities of Watson–Crick and Hoogsteen structures because of an appearance of the aggregation in the samples and the polymer precipitation under Me^{2+} concentration nearly above 5 mM. From mutual dispositions of $3 \rightarrow 2$ branches of the diagram corresponding to the different ions it can be concluded that stabilizing effect of the metal ions on the triplex structure decreases in the following order: $Mg^{2+}>Ni^{2+}>Cd^{2+}$.

The light scattering data obtained for the single-stranded polynucleotide constituents in the presence of the studied dications (Fig. 8) show that an appearance of the aggregation after the polynucleotide melting is conditioned by the intermolecular association of poly(dA) strands. The estimated size of the aggregate, 240 nm, turns out to be comparable with the length of the synthetic poly(dA) strand (polymerization degree of $\sim$500) therefore a random coil cannot be formed by only one poly(dA) strand with Cd^{2+} ions as it was reported earlier for poly(rA) complex in the presence of Cu^{2+} (Shin et al. 1972). Probably, the formation of aggregates arises from intermolecular cross-linkage of poly(dA) by divalent metal cation bridges (Duguid et al. 1995). It occurs under the temperature which is high enough to disorder completely the secondary structure of poly(dA), so that the unpaired nucleic bases can swing out and N7 of adenine become available for the interaction with metal ions. Under the assumptions of a spherical shape for all aggregate particles the coil diameter $D \approx 240$ nm and the number of the monomeric units in the aggregate $\sim 10^7$ were estimated, that allows to calculate the volume occupied by one AMP molecule, which turn out to be equal ~ 0.7 nm^3. This value evidences very dense packing of poly(dA) strands in the aggregate.

As can be seen in Fig. 8, the aggregation process is highly cooperative. Upon reaching the maximal value the light scattering intensity begins to decrease with the further rise of the temperature. It should be noted, that unlike to monophasic light scattering curves registered for the complexes formed by the ions with single-stranded poly(dA), in the case of poly(dA)·poly(dT) biphasic ones are observed (Figs. 6 and 7), that demands explanations. Thus, the thermodynamics of the aggregation of poly(dA) in the presence of Ni^{2+} or Cd^{2+} ions is sufficiently complicated.

It was revealed that magnesium ions don't effect substantially on the Ni^{2+} induced poly(dA) aggregation, since they interact only with polynucleotide phosphate groups and their binding affinity is less than those for Ni^{2+} and Cd^{2+} (Duguid et al. 1993; Eichhorn and Shin 1968). Competition between Mg^{2+} and Ni^{2+} for phosphate binding sites can only increase effective concentration of nickel ions interacting with nucleic bases that resulted in the small shift of light scattering curves to lower temperature range. Absence of an appreciable Mg^{2+} effect on Ni^{2+}-induced aggregation process in the studied polynucleotide systems convincingly evidences that the aggregation occurs as a results of polynucleotide bases cross-linkage by nickel ions. Since Cd^{2+} binding affinity for the bases is substantially higher than that for Ni^{2+}, undoubtedly there will be no Mg^{2+} effect on Cd^{2+}-induced aggregation in studied polynucleotide systems.

Conclusions

The comprehensive diagram of the conformational transitions in the poly(dA)-poly(dT) polynucleotide system in the presence of Ni^{2+} and Cd^{2+} transition metal ions in solutions with 0.1 M NaCl and under polynucleotide concentration of 0.1 mM (in nucleic base pairs or triplets) was constructed. Like Mg^{2+}, the Ni^{2+} ions substantially elevates the temperature of helix-coil transition of poly(dA)·poly(dT) duplex, whereas Cd^{2+} ions slightly decrease it. Both Ni^{2+} and Cd^{2+} ions strongly increase the temperature of triplex-duplex transition in poly(dA)·2poly(dT) system but the Ni^{2+} effect is substantially more pronounced. The branches of the phase diagram do not reach the point of equal stabilities of Watson–Crick and Hoogsteen structures, as was observed earlier for the same polynucleotide system in the presence of alkaline-earth magnesium ions (Zozulya et al. 2003), due to the precipitation of the complexes under Me^{2+} ion concentration nearly above 5 mM. At certain values of the metal ions concentration and temperature an aggregation arises in poly(dA)-poly(dT) systems after their dissociation into single strands, that results in macrocluster formation. The phenomenon is caused by the cross-linkage of poly(dA) strands mediated by the dications. The Cd^{2+} ions (but not Ni^{2+}) induce formation of very stable poly(dA) aggregates which did not disintegrate even upon cooling up to room temperature preventing

the restoration of the duplex or triplex structures. Presumably, the aggregates adopt a configuration of monodisperse coils which diameter was estimated as ~240 nm. No appreciable effect of the near-physiological content of Mg^{2+} ions on Ni^{2+}-induced aggregation in the investigated polynucleotide systems was revealed.

Acknowledgments This work was supported by Government of Ukraine and US Civilian Research and Development Foundation for the Independent States of the Former Soviet Union (CRDF grant UN1-435).

References

Aich P, Labiuk SL, Tari LW, Delbaere LJT, Roesler WJ, Falk KJ, Steer RP, Lee JS (1999) M-DNA: a complex between divalent metal ions and DNA which behaves as a molecular wire. J Mol Biol 294:477–485

Airoldi M, Gennaro G, Giomini M, Giuliani AM, Giustini M (2007) Interaction of the alternating double stranded copolymer poly(dA-dT)·poly(dA-dT) with $NiCl_2$ and $CdCl_2$: solution behavior. J Biomol Struct Dyn 25: 77–84

Alexeev DG, Lipanov AA, Skuratovskii IYa (1987) Poly(dA)·poly(dT) is a B-type double helix with a distinctively narrow minor groove. Nature 325(6107):821–823

Beyersmann D, Hartwig A (2008) Carcinogenic metal compounds: recent insight into molecular and cellular mechanisms. Arch Toxicol 82(8):493–512

Blagoi YuP, Gladchenko GO, Nafie LA, Freedman TB, Sorokin VA, Valeev VA, Ya He (2005) Phase equilibrium in poly(rA)-poly(rU) complexes with Cd^{2+} and Mg^{2+} ions, studied by UV-, IR- and VCD spectroscopy. Biopolymers 78(4):275–286

Chalikian TV, Völker J, Plum GE, Breslauer KJ (1999) A more unified picture for the thermodynamics of nucleic acid duplex melting: a characteriztion by calorimetric and volumetric techniques. Proc Natl Acad Sci USA 96:7853–7858

Conway K, Costa M (1989) Nonrandom chromosomal alterations in nickel-transformed Chinese hamster embryo cells. Cancer Res 49:6032–6038

Costa M (1996) Mechanisms of nickel genotoxicity and carcinogenicity. In: Chang LW (ed) Toxicology of Metals. CRC Press, Boca Raton, FL, pp 245–251

Costa M, Klein CB (1999) Nickel carcinogenesis, mutation, epigenetics, or selection. Environ Health Perspect 107(9):A438–A439

Dally H, Hartwig A (1997) Induction and repair inhibition of oxidative DNA damage by nickel(II) and cadmium(II) in mammalian cells. Carcinogenesis 18:1021–1026

Dechering KJ, Cuelenaere K, Konings RN Leunissen JA (1998) Distinct frequency-distributions of homopolymeric DNA tracts in different genomes. Nucl Acids Res 26:4056–4062

Diekmann S, Zarling DA (1987) Unique poly(dA)·poly(dT) B'-conformation in cellular and synthetic DNAs. Nucl Acids Res 15:6063–6074

Doty P, Steiner RF (1950) Light scattering and spectrophotometry of colloidal solutions. J Chem Phys 18: 1211–1220

Duguid JG, Bloomfield VA, Benevides JM, Thomas GJ (1993) Raman spectroscopy of DNA-metal complexes. I. Interaction and conformational effects of the divalent cationa: Mg, Ca, Sr, Ba, Mn, Co, Ni, Cu, Pd and Cd. Biophys J 65:1916–1928

Duguid JG, Bloomfield VA, Benevides JM, Thomas GJ (1995) Raman spectroscopy of DNA-metal complexes. II. Thermal denaturation of DNA in the presence of Sr^{2+}, Ba^{2+}, Mg^{2+}, Co^{2+}, Ni^{2+}, and Cd^{2+}. Biophys J 69:2623–2640

Eichhorn GL, Shin YAe (1968) Interaction of metal ions with polynucleotides and related compounds. XII. The relative effect of various metal ions on DNA helicity. J Am Chem Soc 90:7323–7328

Filipic M, Fatur T, Vudrag M (2006) Molecular mechanisms of cadmium induced mutagenicity. Hum Exp Toxicol 25: 67–77

Fox KR (1992) Wrapping of genomic polydA·polydT tracts around nucleosome core particles. Nucl Acids Res 20: 1235–1242

Hartwig A (1994) Role of DNA Repair Inhibition in Lead- and Cadmium-induced genotoxicity: a review. Environ Health Perspect 102(Suppl 3):45–50

Huang X, Zhuang Z, Frenkel K, Klein CB, Costa M (1994) The role of nickel and nickel-mediated reactive oxygen species in the mechanism of nickel carcinogenesis. Environ Health Perspect 102(Suppl 3):281–284

IARC Monographs on the Evaluation of Carcinogenic Risk to Humans (1990) vol. 49: Chromium, Nickel and Welding, IARC, Lyon, France

IARC Monographs on the Evaluation of Carcinogenic Risks to Humans (1993) vol. 58: Beryllium, cadmium, mercury, and exposures in the glass manufacturing industry, IARC, Lyon, France

Iyer V, Struhil K (1995) Poly(dA:dT), a ubiquitous promoter element that stimulates transcription via its intrinsic DNA structure. EMBO J 14:2570–2579

Kasprzak KS, Jaruga P, Zastawny T, North SL, Riggs CW, Olinski R, Dizdaroglu M (1997) Oxidative DNA base damage and its repair in kidneys and livers of nickel(II)-treated male F344 rats. Carcinogenesis 18:271–277

Kasprzak KS, Sunderman FW Jr, Salnikow K (2003) Nickel carcinogenesis. Mutat Res 533(1–2):67–97

Kasyanenko NA, Diakonova NE, Frisman EV (1989) Investigation of DNA molecular conformation under its interaction with divalent ions in solution. Mol Biol 23:975–982

Kim J, Soh J (2009) Cadmium-induced apoptosis is mediated by translocation of AIF to the nucleus in rat testes. Toxicol Lett 188:45–51

Lee YW, Klein CB, Kargacin B, Salnikow K, Kitahara J, Dowjat K, Zhitkovitch A, Christie NT, Costa M (1995) Carcinogenic nickel silences gene expression by chromatin condensation and DNA hypermethylation: a new model for epigenetic carcinogens. Mol Cell Biol 15(5):2547–2557

López E, Arce C, Oset-Gasque MJ, Cañadas S, González MP (2006) Cadmium induces reactive oxygen species generation and lipid peroxidation in cortical neurons in culture. Free Radic Biol Med 40(6):940–951

Lustig AJ, Petes TD (1984) Long poly(A) tracts in the human genome are associated with the Alu family of repeated elements. J Mol Biol 180:753–759

Nelson HC, Finch JT, Luisi BF, Klug A (1987) The structure of an oligo(dA)·oligo(dT) tract and its biological implications. Nature 330(6145):221–226

Saenger W (1984) Principles of nucleic acid structure. Springer, New York

Salnikow K, Cosentino S, Klein C, Costa M (1994) The loss of thrombospondin transcriptional activity in nickel-transformed cells. Mol Cell Biol 14:851–858

Segal E, Widom J (2009) Poly(dA:dT) tracts: major determinants of nucleosome organization. Curr Opin Struct Biol 19:65–71

Seoane AI, Dulout FN (2001) Genotoxic ability of cadmium, chromium and nickel salts studied by kinetochore staining in the cytokinesis-blocked micronucleus assay. Mutat Res Genet Toxicol Environ Mutagen 490(2):99–106

Shin YA, Heim JM, Eichhorn GL (1972) Interaction of metal ions with polynucleotides and related compounds. XX. Control of the conformation of polyriboadenylic acid by divalent metal ions. Bioinorg Chem 1:149–163

Sirover MA, Loeb LA (1976) Metal activation of DNA synthesis. Biochem Biophys Res Commun 70:812–817

Sorokin VA, Valeev VA, Gladchenko GO, Sysa IV (1997) Interaction of divalent cadmium ions with nucleotides and native DNA. Biophysics 42(1):105–111

Sorokin VA, Valeev VA, Gladchenko GO, Degtyar MV, Blagoi YuP (2001) Ni^{2+} ion effect on conformations of single-, double- and three-stranded homopolynucleotides containing adenine and uracil. Macromol Biosci 1:191–203

Sorokin VA, Valeev VA, Usenko EL, Blagoi YuP (2007) Effect of Cd^{2+} ions on conformational equilibrium of three-stranded polyU·polyA·polyU polynucleotide under near-physiological conditions. Biopolym Cell 23(5): 433–440

Sorokin VA, Usenko EL, Valeev VA (2008) Mg^{2+} and Ni^{2+} ion Effects on phase transitions in AU and A2U under conditions close to physiological ones. IFMBE Proc 20(1):628–631

Sorokin VA, Valeev VA, Usenko EL (2009) Phase diagram of Ni^{2+} ions complexes with polyU·polyA·polyU. Biopolym Cell 25(3):218–225

Souza HKS (2010) Calf thymus DNA–metal ions interactions: calorimetric and spectroscopic thermal studies. Thermochim Acta 501:1–7

Thrierr JC, Leng M (1972) A study of complexes between polyriboadenylic acid and polyribouridylic acid: formation and structure. Biochimica et Biophysica Acta (BBA) Nucleic Acids and Protein Synthesis 272(2): 238–251

Waalkes MP (2000) Cadmium carcinogenesis in review. J Inorg Biochem 79:241–244

Waalkes MP and Misra RR (1996) Cadmium carcinogenicity and genotoxicity. In: Chang LW (ed) Toxicology of metals. CRC Press, Boca Raton, FL, pp 231–244

Zozulya VN, Nesterov AB, Ryazanova OA, Blagoi YuP (2003) Conformational transitions and aggregation in poly(dA)-poly(dT) system induced by Na^{+} and Mg^{2+} ions. Int J Biol Macromol 33(4–5):183–191